Intramolecular Charge-Transfer Process Based on Dicyanomethylene-4H-pyran Derivative: An Integrated Operation of Half-Subtractor and Comparator

ARTICLE *in* THE JOURNAL OF PHYSICAL CHEMISTRY C · MAY 2008

Impact Factor: 4.77 · DOI: 10.1021/jp0777162

6 AUTHORS, INCLUDING:

Zhiqian Guo
East China University of Science and Technol…
49 PUBLICATIONS **2,101** CITATIONS
SEE PROFILE

Weihong Zhu
East China University of Science and Technol…
148 PUBLICATIONS **5,526** CITATIONS
SEE PROFILE

Intramolecular Charge-Transfer Process Based on Dicyanomethylene-4*H*-pyran Derivative: An Integrated Operation of Half-Subtractor and Comparator

Zhiqian Guo, Ping Zhao, Weihong Zhu,* Xiaomei Huang, Yongshu Xie, and He Tian*

Key Laboratory for Advanced Materials and Institute of Fine Chemicals, East China University of Science & Technology, Shanghai 200237, P. R. China

Received: September 26, 2007; In Final Form: January 31, 2008

Integration of simple logic gates into combinational circuits is a crucial step for the performance of arithmetic systems and working automation. A half-subtractor has been reported in combination with a comparator based on the intramolecular charge transfer (ICT) process resulting from hosting two different guests with the binding of Zn^{2+} and the deprotonation of phenolic hydroxyl groups in an unimolecular system. The corresponding spectral shifts in absorption and a variation in fluorescence intensity were well elucidated. An XOR (exclusive OR) logic gate generates the difference digit of the half-subtractor reading at 445 nm, and two INHIBIT logic gates, which are basically AND gates with one of the inputs inverted through a NOT function, are achieved for the borrow digit of the half-subtractor when the output signals are monitored at 400 and 525 nm. Taken together, the comparison and subtraction operations are practically performed in parallel without mutual interference due to the same inputs and different outputs within the same molecule system.

Introduction

Remarkable progress in the development of molecular logic gates has brought chemists closer to the realization of a molecular scale calculator[1,2] since the first report of a molecular AND logic gate by de Silva et al.[3] Many individual logic gates, such as OR, NOT, XOR, XNOR, INHIBIT, NOR, and NAND, have been defined on the basis of spectral variations of molecular systems in response to external stimulations.[4−10] Up to now, only a few reported examples can implement combinational logic circuits (XOR-INH, AND-INH, XOR-AND)[11] in a unimolecular entity. Recently, Wang et al. have realized multiply configurable optical-logic systems based on cationic conjugated polymer/DNA assemblies.[7b]

Integration of simple logic gates into combinational circuits is a crucial step for the performance of arithmetic systems and working automation.[12] Recently, a molecular arithmetic system based on fluorescein was demonstrated by Shanzer et al., capable of performing a full scale of binary addition and subtraction algebraic operations.[2h] However, improving the processing power of molecules still remains a great challenge for molecular logic and arithmetical simulations. For instance, a half-subtractor can implement the combinatorial logic circuit that can carry out elementary subtraction through the XOR gate to generate the difference digital (D) and the INHIBIT gate to generate the borrow digital (B). Moreover, a half-subtractor performing an algebraic subtraction operation might be complicated over a half-adder, since the relative magnitudes of subtrahend and minuend are required to be compared.[11g,11i,13] Therefore, an integrated operation of half-subtractor and comparator could become more feasible in the general subtraction process. Bearing these considerations in mind, herein we designed a V-shaped molecule of 2-{2-{4-[bis(pyridin-2-ylmethyl)amino]styryl}-6-(4-hydroxystyryl)-4*H*-pyran-4-ylidene}malononitrile (DADPP, Figure 1) to realize a combination of half-subtractor and comparator based on the intramolecular charge transfer (ICT) process. The two receptors of DADPP host different guests with the binding of Zn^{2+} and the deprotonation of phenolic hydroxyl groups, resulting in a corresponding spectral shift in absorption and a variation in fluorescence intensity. In this receptor$_1$−chromophore−receptor$_2$ system, the corresponding spectral shift results from the charge separation in the excited chromophore by a shift of electron density when DADPP hosts different guests (Figure 1).[2j] Several aspects, such as easy synthesis of target molecules, low interferences between logic gates by the unimolecular implementation, and resetting capability, are addressed in detail to afford a way of connecting general subtraction operations. More preferably, the comparison and subtraction operations are practically performed in parallel without mutual interference due to the same inputs and different outputs in the molecule system.

Results and Discussion

Synthesis. DADPP has two receptors, an aromatic unit possessing bis(2-pyridyl-methyl)amine (DPA) moiety and a phenolic moiety, via double bonds as bridges to incorporate a dicyanomethylene-4*H*-pyran unit as the chromophore. DADPP can be conveniently synthesized by the condensation of 4-hydroxybenzaldehyde and 4-[bis(pyridin-2-yl-methyl)amino]benzaldehyde with 4-dicyanomethylene-2,6-dimethyl-4*H*-pyran in about 35% yield. Its chemical structure is fully characterized by ^{1}H NMR, ^{13}C NMR, and high-resolution mass spectrometry (HRMS) in the Experimental section. In ^{1}H NMR of DADPP, the characteristic coupling constant (J = 16.0 Hz) of protons (a) and (b) and (c) and (d) are indicative of the predominant *trans*-isomer.

pH Effect on the Spectral Properties of DADPP. The ICT mechanism has been widely exploited for ion sensing and molecular switching.[2f] Indeed, we have constructed crossword

* To whom correspondence should be addressed. E-mail: whzhu@ecust.edu.cn (W.H.Z.); tianhe@ecust.edu.cn (H.T.). Fax: (+86) 21-6425-2758.

10.1021/jp0777162 CCC: $40.75
Published on Web 04/10/2008

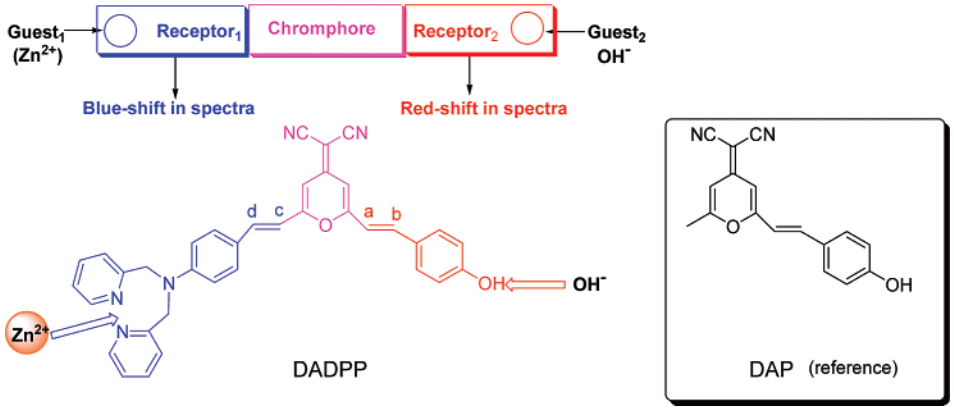

Figure 1. DADPP hosting two different guests and reference compound DAP.

TABLE 1: Truth Table for Half-Subtractor Based on the Changes in Absorbance

input		output			half-subtractor	
Zn^{2+} input (*a*)	OH^- input (*b*)	INHIBIT (B) 400 nm	XOR (D) 445 nm (negative logic)	INHIBIT (B) 525 nm	*a* − *b* 525/445 nm	*b* − *a* 400/445 nm
0	0	0 (0.620)	0 (1.105)	0 (0.361)	00	00
1	0	1 (0.891)	1 (0.989)	0 (0.081)	01	11
0	1	0 (0.660)	1 (0.989)	1 (0.766)	11	01
1	1	0 (0.554)	0 (1.103)	0 (0.373)	00	00

puzzles and logic memory based on the ICT process.[14] In a "push−pull" system, one terminal tends to be electron rich and the other electron poor so that the consequent change in dipole moment can result in a Stokes shift.[5,15a] When the electron-donating character of the receptor moiety is reduced by binding specific target species, hypsochromic shifts in both absorption and fluorescence spectra are expected. Conversely, if target species promote the electron-donating character of the receptor moiety, the absorption and fluorescence spectra should exhibit bathochromic shifts.[15]

DADPP as a derivative of the well-known laser dye 4-dicyanomethylene-2-methyl-6-[4-(dimethylamino)styryl]-4*H*-pyran (DCM) is a typical A-π-D type with a broad absorption band resulting from an ultrafast ICT process.[16] The pH-dependent changes of DADPP in the absorption spectra and the emission spectra were investigated and are shown in Figure 2. The decrease of pH induces the protonation of the amino group of the DPA unit in DADPP. The presence of an isobestic point at 480 nm clearly displays an equilibrium process corresponding to free DADPP and protonated DADPP ($DADPP^+$) with a slight hypsochromic shift and an increase in absorbance intensity during pH changes from 2.75 to 7.30 (Figure 2A). In contrast, adding a strong base (NaOH) can deprotonate the phenolic hydroxyl group of DADPP to become its phenolate as $DADPP^-$. Similarly, the isobestic point at 460 nm in the pH range from 7.30 to 11.27 also reveals that only two species coexist corresponding to free DADPP and $DADPP^-$ (Figure 2B). Clearly, the variation in absorption spectra stimulated with pH results from the change of electron donor units via protonation or deprotonation.

Additionally, the fluorescence intensity of free DADPP at 615 nm was gradually increased from pH 7.30 to 2.75 (Figure 2C) with a pK_a value of 4.6. Such fluorescent intensity variation with pH is quite complicated and unexpected. However, it is definitely dependent on the competition between two channels under pH changing from 7.30 to 2.75: (i) the ICT process from the aniline nitrogen to the chromophore of dicyanomethylene-4*H*-pyran (*fluorescence enhancement effect*) and (ii) the photoinduced electron transfer (PET) process from the aniline nitrogen to the nitrogen atoms of pyridine within the DPA group (*fluorescence quenching effect*). We consider that, with changing the pH value from 7.30 to 2.75, the PET process from the aniline to the nitrogen atoms of pyridine within the DPA group is decreasing with respect to the ICT process. That is, the fluorescence enhancement with decreasing pH value can be attributed to a block of the PET process from the aniline to the pyridine, which is well consistent with the nitrogen atom of pyridine being both an ion receptor and quencher of PET.[17a]

As is known, the phenolic hydroxyl group is moderately π electron-donating with respect to the amine nitrogen atom of the DPA group. The fluorescence of the reference compound DAP (Figure 1) is very weak, testifying this effect, in which the trend from electron rich to electron poor is weak.[18] However, when the phenolic hydroxyl group of DADPP is deprotonated as the phenolate ($DADPP^-$) in the presence of a strong base, the negative charge on oxygen in the phenolate group leads to a decrease in the attractive electronic-nuclear interaction, raising the levels of atomic orbits on oxygen.[19a] Thus, upon deprotonation, PhO^- in $DADPP^-$ becomes a strong π electron donor in the quinoidal resonance form with alternating double and single C−C bonds, undergoing efficient ICT to the dicyanomethylene-4*H*-pyran acceptor,[19] which stabilizes the excited state with a resulting spectral red-shift. As a matter of fact, the absorption titration reveals that the stepwise addition of a strong base causes a bathochromic shift by about 42 nm from 442 to 484 nm (Figure 2B).

Zn^{2+} Binding Effect on the Spectral Properties of DADPP. DPA is the most widely used ligand for Zn^{2+} binding.[17] In DADPP, the DPA moiety acts as an electron-donating substituent whose donor character strongly depends on cation complexation. As illustrated in Figure 3A, the presence of an isobestic point at 437 nm clearly reveals that only two species coexist corresponding to free DADPP and the zinc complex ($DADPP\text{-}Zn^{2+}$). The corresponding absorption spectra also exhibit an obvious hypsochromic shift from 442 to 415 nm upon stepwise addition of Zn^{2+} to DADPP, with the accompanied color change from orange yellow to light green being clearly observed by naked eyes (Figure 4), indicating that the electron-

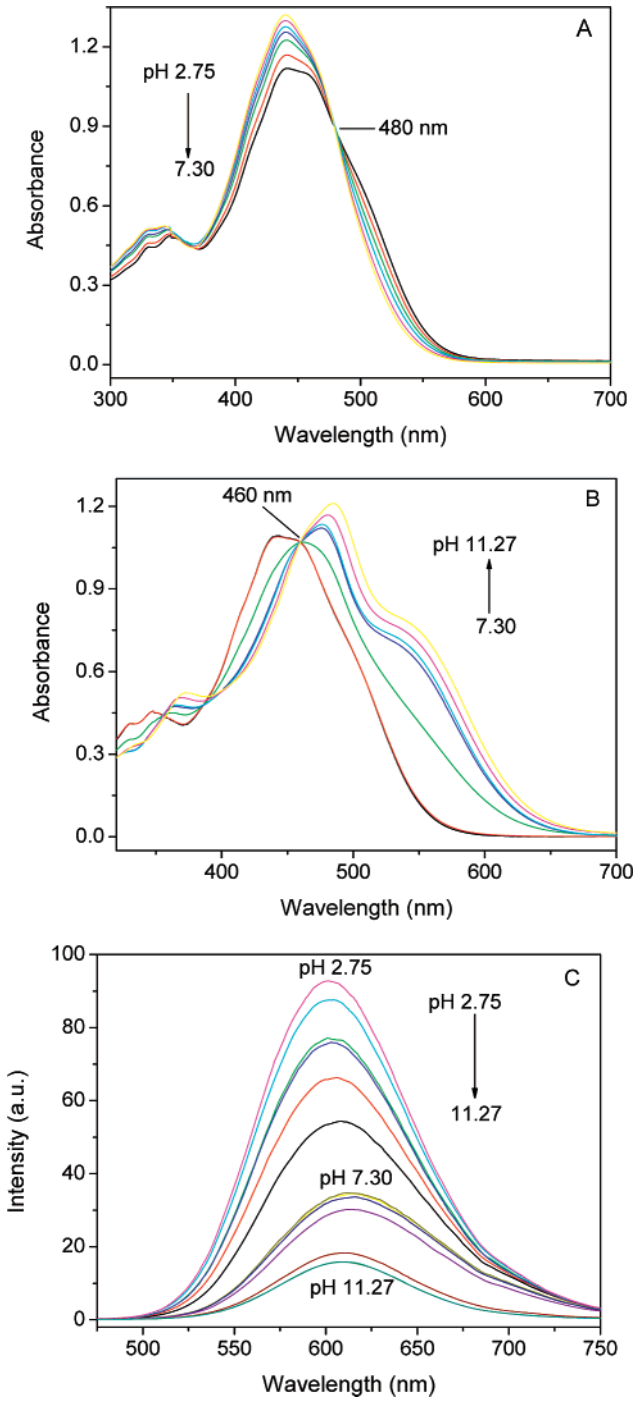

Figure 2. pH titration profiles of DADPP (10 μM) in ethanol/water solutions (1:9, v/v): (A) absorption spectra change with pH from 2.75 to 7.30; (B) absorption spectra change with pH from 7.30 to 11.27; and (C) emission spectra change with pH from 2.75 to 11.27 (λ_{ex} = 445 nm). The pH value was adjusted by $HClO_4$ and NaOH.

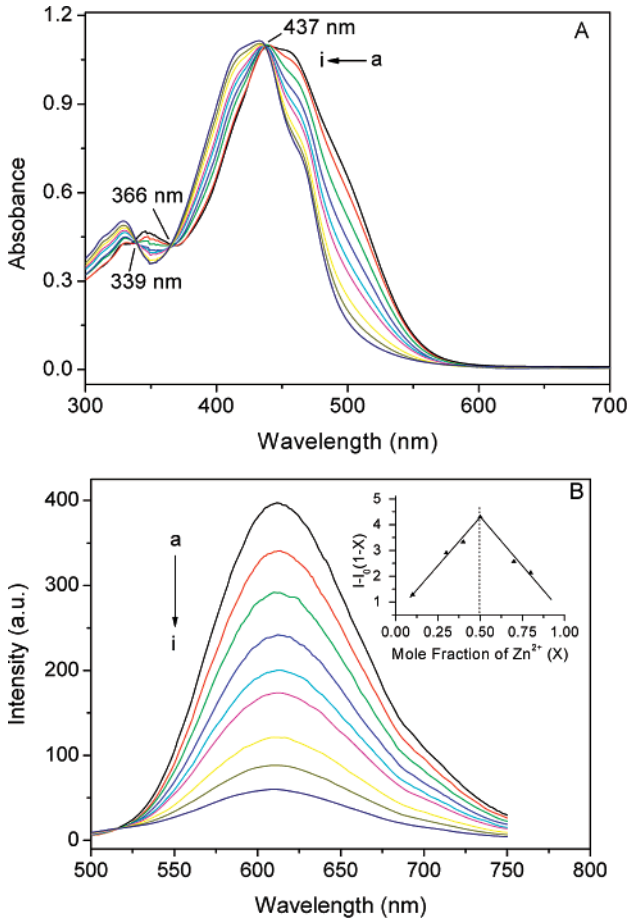

Figure 3. (A) Absorption spectra of DADPP (20 μM) in a mixture of H_2O/C_2H_5OH (1:9, v/v) upon addition of Zn^{2+}; [Zn^{2+}] = 0, 2, 4, 8, 12, 16, 18, 20, and 40 μM from a to i with three isobestic points of 339, 366, and 437 nm. (B) Emission spectra of DADPP (20 μM) in a mixture of H_2O/C_2H_5OH (1:9, v/v) upon addition of Zn^{2+}; [Zn^{2+}] = 0, 2, 4, 8, 12, 16, 18, 20, and 40 μM from a to i (λ_{ex} = 445 nm). (Inset) Job's plot of DADPP (the total concentration of DADPP and Zn^{2+} is 50.0 μM).

Figure 4. Color change of DADPP (20 μM) in a mixture of H_2O/C_2H_5OH (1:9, v/v). From left to right: DADPP (DADPP alone), DADPP-Zn^{2+} (in the presence of 40 μM $ZnCl_2$), $DADPP^-$ (in the presence of 0.3 mM NaOH), and $DADPP^-$-Zn^{2+} (in the presence of 40 μM $ZnCl_2$ and 0.3 mM NaOH).

donating character of the amine nitrogen atom of the DPA group is decreased, thus resulting in a decrease in ICT efficiency by coordination with Zn^{2+}.[14b,17d] However, the interaction only shows a slight hypsochromic shift in the emission signature and an almost complete quenching of fluorescence, which can be attributed to the locally excited (LE) state and relaxed intramolecular charge transfer (RICT) of DADPP.[16] Therefore, the fluorescence spectrum is thus only slightly affected, since most of the contribution to fluorescence is still from DADPP.[14a] On the other hand, the excitation spectra of DADPP, which show a drastic hypsochromic shift from 485 to 440 nm, also confirm the blue-shift of the ICT effect (Figure S1 in the Supporting Information). Both the linear decrease of fluorescence intensity within the equivalent range of the Zn^{2+} ion and its Job's plot indicate that DADPP forms a 1:1 complex with the Zn^{2+} ion (Figure 3B), whose association constant (K_{ass}) is determined to be about 1.4 × 10^5 M^{-1} by fluorometric titration curves.[20]

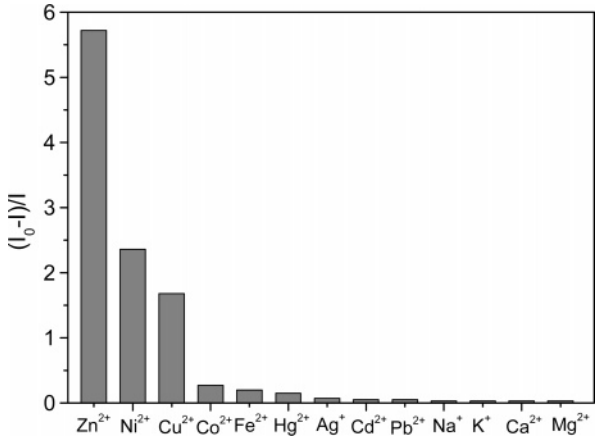

Figure 5. Fluorescent intensity change of DADPP (20 μM) in a mixture of H_2O/C_2H_5OH (1:9, v/v) in the presence of various metal ions: Zn^{2+} (40 μM), Ni^{2+} (40 μM), Cu^{2+} (40 μM), Co^{2+} (100 μM), Fe^{2+} (100 μM), Hg^{2+} (100 μM), Ag^{+} (100 μM), Cd^{2+} (100 μM), Pb^{2+} (100 μM), Na^{+} (100 μM), K^{+} (100 μM), Ca^{2+} (100 μM), and Mg^{2+} (100 μM). The bar represents the fluorescent intensity change ($(I_0 - I)/I$), in which I_0 indicates the fluorescent intensity of free sensor DADPP.

Moreover, the selectivity and sensitivity of DADPP were performed with various metal ions. As illustrated in Figure 5, the $(I_0 - I)/I$ values in the presence of Ni^{2+} and Cu^{2+} show a slight disturbance to Zn^{2+} in the emission spectra of DADPP. The addition of other metal ions such as Cd^{2+}, Co^{2+}, Fe^{2+}, Hg^{2+}, Ag^{+}, Pb^{2+}, Na^{+}, K^{+}, Ca^{2+}, and Mg^{2+} produce a nominal change in the emission spectra due to their low affinity with DADPP.

The response of DADPP to Zn^{2+} in the absence and presence of a base was also investigated. As shown in Figure S2 in the Supporting Information, the absorption peak shifts from 478 to 442 nm upon the addition of Zn^{2+} to DADPP in the presence of excess base. It implies that Zn^{2+} coordination with the DAP unit occurs prior to the reaction with OH^{-}, resulting in DADPP^{-}-Zn^{2+}. On the other hand, a shift from 415 to 442 nm in the absorption spectra can be seen upon adding the base to DADPP in the presence of Zn^{2+} (Figure S3 in the Supporting Information). When DADPP hosts two different guests with the binding of Zn^{2+} and the deprotonation of phenolic hydroxyl groups, it shows almost the completely same shape or color as net DADPP (Figure 4) in that the two different receptors are located at the opposite poles of the chromophore, thus affording the opposite spectral effect.[5] As a result, the corresponding color and schematic interconversion of four different states are illustrated in Figures 4 and 6, respectively.

An Integrated Operation of Half-Subtractor and Comparator. To take advantage of spectral effects resulting from the varying electron-donating character of the receptor moiety in the ICT mechanism, the XOR and INHIBIT logic operations can be constructed on the basis of the changes in absorbance as an output and two chemicals of Zn^{2+} and OH^{-} as inputs. As illustrated in Figure 7, it is found that the output signals are low with either one of two inputs at 445 nm and the threshold is kept at 1.0. Furthermore, two simultaneous inputs in the form of Zn^{2+} and OH^{-} convert DADPP to DADPP^{-}-Zn^{2+}. Thus, these observations are correlated with an XNOR logic gate as its output signal is *off* when either input is *on* but *on* when the inputs are both *on* or both *off*. When the output signals in the absorption spectra are monitored at 400 and 525 nm, the two INHIBIT logic gates are also obtained (the threshold for both is at 0.70, Table 1). Moreover, XNOR and XOR logic operators are "duals" of each other. It is reasonable to choose an application of negative only on the outputs because of the different kinds of inputs. Thus, following this procedure for the outputs at 445 nm, the XNOR gate is effectively transformed into an XOR gate. Now, an XOR logic gate generates the difference digit of the half-subtractor reading at 445 nm, and two INHIBIT logic gates are achieved for the borrow digit of the half-subtractor when the output signals are monitored at 400 and 525 nm. The function of the half-subtractor represented by conventional electronic symbols is illustrated in Figure 8.

In DADPP emission spectra, an XNOR logic operation can also be expressed by monitoring the fluorescence intensity at 615 nm. The output is annihilated in the *off* state in the presence of either Zn^{2+} or OH^{-}. The fluorescence of DADPP-Zn^{2+} is quenched as a result of the coordination of Zn^{2+} with the amine

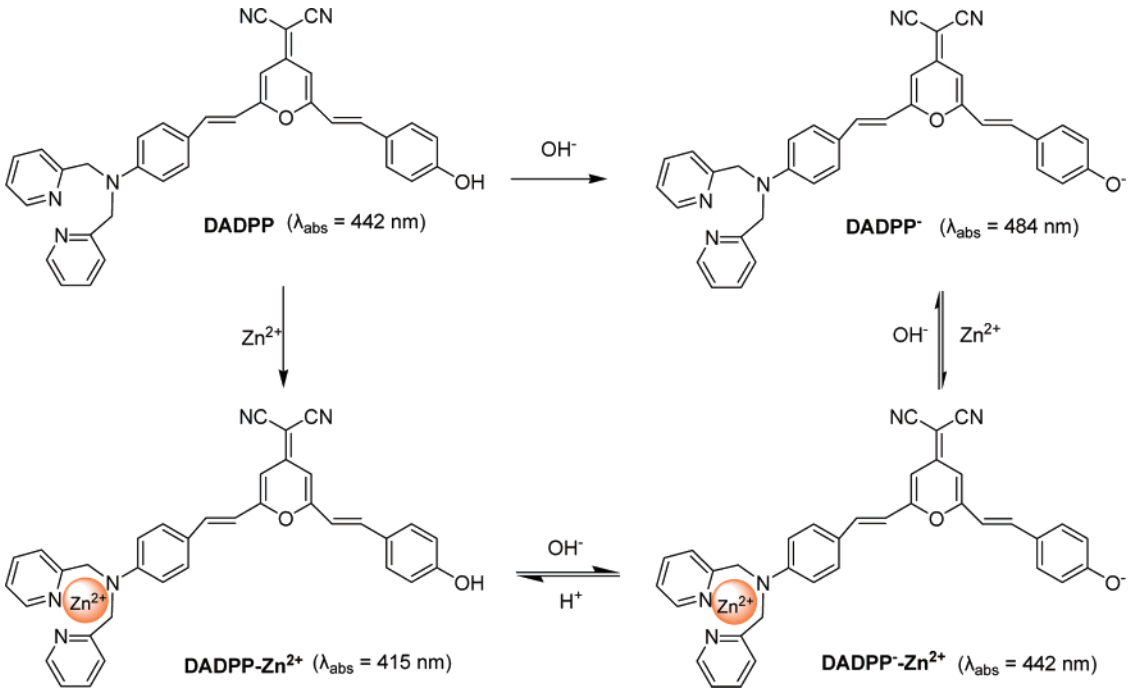

Figure 6. Schematic interconversions of different states with corresponding absorption peaks.

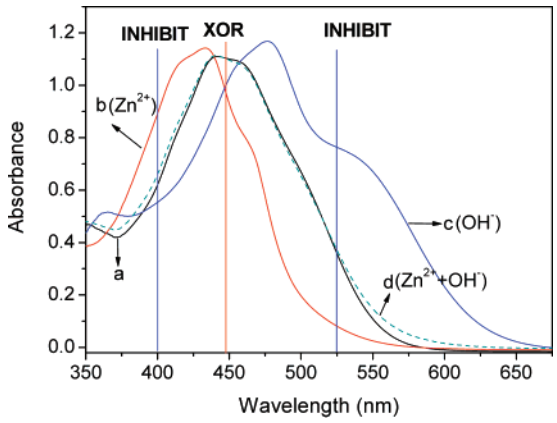

Figure 7. Absorption spectra of DADPP (20 μM) in a mixture of H_2O/C_2H_5OH (1:9, v/v) upon addition of (a) DADPP alone, (b) 2 equiv of Zn^{2+}, (c) 15 equiv of OH^-, and (d) 2 equiv of Zn^{2+} + 15 equiv of OH^-.

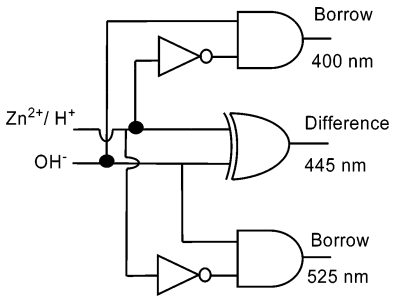

Figure 8. Logic diagram of the half-subtractor. The "difference" and "borrow" outputs were collected at three different wavelengths of 400, 445, and 525 nm.

nitrogen atom of the DPA group, which decreases the electron-donating character with respect to the rest of the molecule. Additionally, the fluorescence efficiency of $DADPP^-$ is also decreased, which might be attributed to the vibrational-loss mechanism in a protic solvent.[21] It is in the *on* state as DADPP alone, Zn^{2+}, OH^-, and Zn^{2+} and OH^- inputs are present in Figure 9. Thus, this could also perform an XNOR logic gate operation in DADPP emission (with the threshold at 60). Notably, the presented XOR gate based on fluorescence outputs in Figure 9 (negative logic) can also replace the absorption spectra output at 445 nm in Figure 7 to mimic a more realistic half-subtractor with a moderate threshold at 60.

Generally, there are two basic types of digital comparators: identity comparators and magnitude comparators.[22] Identity comparators indicate whether two inputs are equal. The XOR gate is actually an identity comparator. Magnitude comparators express the relative magnitude of two inputs, if they are not equal, which input is larger or smaller (Table 2 and Figure S4 in the Supporting Information).[23] Thus, a molecular digital comparator can be constructed at 525 nm in absorption spectra and at 615 nm in emission spectra. If the output *eq* of the comparator is 1, then $b = a$; if the output *gt* is 1, then $b > a$; if both *gt* and *eq* are 0, then $b < a$.

There are two INHBIT logic gates with different responses to the inputs in the absorption mode of DADPP, so the order of minuend and subtrahend can be exchanged according to the requirement. The $(a - b)$ and $(b - a)$ algebraic operation can be differentiated by a magnitude comparator mentioned above. Assumed to obtain the difference of $(b - a)$, the relative magnitudes of b and a should be compared first by a comparator.

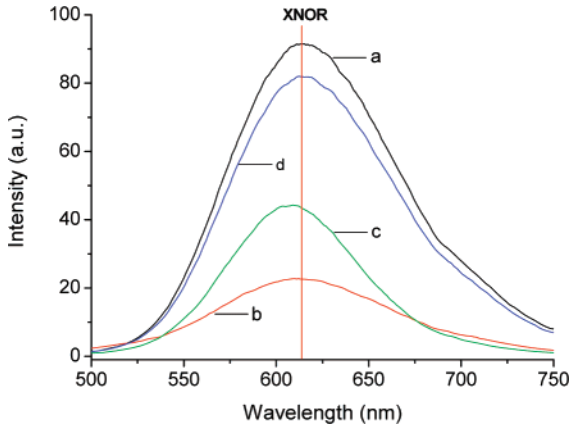

Figure 9. Emission spectra of DADPP (2.0×10^{-5} M) in a mixture of H_2O/C_2H_5OH (1:9, v/v) upon addition of (a) DADPP alone, (b) 2 equiv of Zn^{2+}, (c) 15 equiv of OH^-, and (d) 2 equiv of Zn^{2+} + 15 equiv of OH^- (λ_{ex} = 445 nm).

TABLE 2: Symbol and Truth Table for the Operation Digital Comparator in Absorption and Emission Modes

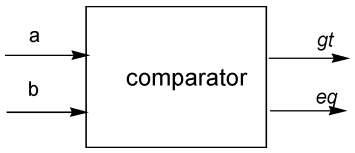

	input		output	
comparator	Zn^{2+} input (a)	OH^- input (b)	*gt* (Abs) 525 nm	*eq* (Flu) 615 nm
$b = a$	0	0	0 (0.361)	1 (92)
$b < a$	1	0	0 (0.081)	0 (22)
$b > a$	0	1	1 (0.766)	0 (42)
$b = a$	1	1	0 (0.373)	1 (82)

The INHBIT gate at 400 nm integrates with the XOR gate at 445 nm to perform the $(b - a)$ algebraic operation, and $(b - a) = 1$. However, the half-subtractor combined with the INHBIT gate at 525 nm is chosen to execute the $(a - b)$ algebraic operation for the positive algebraic operation and $(a - b) = 1$. In this process, $(b - a) = -1$ is obtained by adding the minus sign to the difference according to the output of comparator.[13] So the comparison and the subtraction operation are practically performed in parallel without mutual interference due to the same inputs and different outputs in this molecule system.

It should be noted that choosing excess Zn^{2+} (2 equiv) and OH^- (15 equiv) as two inputs is for the sake of a more obvious change in the spectra. The addition of H^+ can also replace the addition of Zn^{2+} after the first cycle of the interconversion of $DADPP^-$, $DADPP^-$-Zn^{2+}, and DADPP-Zn^{2+}. Moreover, these cycles can be repeated with the base and acid (Figure S5 in the Supporting Information).

Conclusion

In summary, a half-subtractor has been successfully constructed in combination with a comparator. The spectral properties of DADPP binding two guests (Zn^{2+} and OH^-) based on the ICT process have been investigated. The two receptors of DADPP host different guests with the binding of Zn^{2+} and the deprotonation of phenolic hydroxyl groups, resulting in a corresponding spectral shift in the absorption spectra and a variation in fluorescence intensity. Notably, the combinatorial logic circuit affords a way of connecting general subtraction

operations implemented on a single molecule that could enhance the processing power of the molecule processor effectively.

Experimental Section

General Information. All solvents were of analytical grade. The intermediates of 4-(dicyanomethylene)-2-isopropyl-6-methyl-4*H*-pyran and 4-[bis(pyridin-2-yl-methyl)amino]benzaldehyde were prepared by the established literature procedure.[17c,24] ^{1}H NMR and ^{13}C NMR spectra in $CDCl_3$ or DMSO-d_6 were measured on a Bruker AV-400 spectrometer with tetramethylsilane (TMS) as the internal standard. Mass spectra were measured on a Micromass LCT instrument. UV−vis spectra were obtained using a Varian Cary 500 spectrophotometer (1 cm quartz cell) at 25 °C. Fluorescent spectra were recorded on a Varian Cary Eclipse fluorescence spectrophotometer (1 cm quartz cell) at 25 °C.

2-{2-(4-Hydroxystyryl)-6-methyl-4*H*-pyran-4-ylidene}-malononitrile (Compound DAP). In a 100 mL round-bottomed flask equipped with a stir bar, reflux condenser, and nitrogen bubbler was added 4-(dicyanomethylene)-2,6-dimethyl-4*H*-pyran (2.0 g, 11.6 mmol), 4-hydroxybenzaldehyde (0.8 g, 6.5 mmol), toluene (60 mL), piperidine (1 mL), and acetic acid (0.5 mL). The mixture was refluxed for 8 h and then cooled. The solvent was evaporated in vacuo. The crude solid was purified by column chromatography on silica gel eluting with dichloromethane/methanol 20:1 (v/v) to afford a yellow solid. Yield: 65%. ^{1}H NMR (400 MHz, $CDCl_3$, ppm): δ 2.41 (s, 3H, $-CH_3$), 6.55 (d, 1H, $J = 2.4$ Hz, pyran-H), 6.57 (d, 1H, $J = 16.0$ Hz, alkene-H), 6.65 (d, 1H, $J = 2.4$ Hz, pyran-H), 6.90 (d, 2H, $J = 7.6$ Hz, phenyl-H), 7.39 (d, 1H, $J = 16.0$ Hz, alkene-H), 7.45 (d, 2H, $J = 7.6$ Hz, phenyl-H).

2-{2-{4-[Bis(pyridin-2-ylmethyl)amino]styryl}-6-(4-hydroxystyryl)-4*H*-pyran-4-ylidene}malononitrile (Compund DADPP). In a 50 mL round-bottomed flask equipped with a stir bar, reflux condenser, and nitrogen bubbler was added compound DAP (0.68 g, 2.47 mmol), 4-[bis(pyridin-2-yl-methyl)amino]benzaldehyde (0.85 g, 2.83 mmol), toluene (50 mL), piperidine (1 mL), and acetic acid (0.5 mL). The resulting mixture was refluxed for 10 h and then cooled. The solvent was evaporated in vacuo. The crude solid was purified by column chromatography on silica gel eluting with dichloromethane/methanol 20:1 (v/v) to afford a red solid. Yield: 35%. ^{1}H NMR (400 MHz, DMSO-d_6, ppm): δ 4.90 (s, 4H, $-NCH_2$), 6.64 (d, 1H, $J = 1.6$ Hz, pyran-H), 6.70 (d, 1H, $J = 2.0$ Hz, pyran-H), 6.72 (d, 2H, $J = 8.8$ Hz, phenyl-H), 6.82 (d, 2H, $J = 8.4$ Hz, phenyl-H), 6.96 (d, 1H, $J = 16.0$ Hz, alkene-H), 7.08 (d, 1H, $J = 16.0$ Hz, alkene-H), 7.27 (m, 2H, pyridine-H), 7.30 (d, 2H, $J = 8.0$ Hz, pyridine-H), 7.52 (d, 2H, $J = 8.4$ Hz, phenyl-H), 7.57 (d, 1H, $J = 16.0$ Hz, alkene-H), 7.59 (d, 1H, $J = 16.0$ Hz, alkene-H), 7.61 (d, 2H, $J = 8.4$ Hz, phenyl-H), 7.73 (t × d, 2H, $J = 7.6$, 1.6 Hz, pyridine-H), 8.55 (d, 2H, $J = 4.4$ Hz, pyridine-H). ^{13}C NMR (100 MHz, $CDCl_3$, ppm): δ 59.82, 61.89, 110.35, 110.90, 117.55, 118.71, 120.78, 120.95, 121.20, 126.38, 127.53, 128.37, 131.37, 135.08, 135.30, 142.08, 142.85, 143.45, 154.56, 155.00, 161.04, 163.38, 164.29, 164.67, 164.86. Mass spectrometry (ESI positive ion mode for M + H): calcd, 562.2219; found, 562.2243.

Acknowledgment. This work was financially supported by NSFC/China, National Basic Research 973 Program (2006CB806200), Education Committee of Shanghai and Scientific Committee of Shanghai. W.H.Z. also thanks the Program for New Century Excellent Talents in University (NCET-06-0418) and Shanghai Shuguang Project (07SG34).

Supporting Information Available: Excitation spectra, absorption peak shifts in the presence of excess base or 2.0 equiv of Zn^{2+}, cycles of DADPP repeated with base and acid, ^{1}H NMR, ^{13}C NMR, and HRMS spectra of DADPP, and symbol and truth table for the single-bit magnitude comparator. This material is available free of charge via the Internet at http://pubs.acs.org.

References and Notes

(1) (a) Ball, P. *Nature* **2007**, *445*, 362−363. (b) Green, J. E.; Choi, J. W.; Boukai, A.; Bunimovich, Y.; Johnston-Halperin, E.; Delonno, E.; Luo, Y.; Sheriff, B. A.; Xu, K.; Shin, Y. S.; Tseng, H.-R.; Stoddart, J. F.; Heath, J. R. *Nature* **2007**, *445*, 414−417. (c) Margulies, D.; Felder, C. E.; Melman, G.; Shanzer, A. *J. Am. Chem. Soc.* **2007**, *129*, 347−354.

(2) For recent advances, see (a) de Silva, A. P.; McClenaghan, N. D.; McCoy, C. P. In *Molecular Switches*; Feringa, B. L., Ed.; Wiley-VCH: Weinheim, 2000. (b) Balzani, V.; Venturi, M.; Credi, A. *Molecular Devices and Machines*; Wiley-VCH: Weinheim, 2003. (c) Raymo, F. M. *Adv. Mater.* **2002**, *14*, 401−414. (d) de Silva, A. P.; McClenaghan, N. D. *Chem.—Eur. J.* **2004**, *10*, 574−586. (e) Balzani, V.; Credi, A.; Venturi, M. *ChemPhysChem* **2003**, *3*, 49−59. (f) Callan, J. F.; de Silva, A. P.; Magri, D. C. *Tetrahedron* **2005**, *61*, 8551−8588. (g) Margulies, D.; Melman, G.; Shanzer, A. *Nat. Mater.* **2005**, *4*, 768−771. (h) Margulies, D.; Melman, G.; Shanzer, A. *J. Am. Chem. Soc.* **2006**, *128*, 4865−4871. (i) de Silva, A. P.; Uchiyama, S.; Vance, T. P.; Wannalerse, B. *Coord. Chem. Rev.* **2007**, *251*, 1623−1632. (j) de Silva, A. P.; Uchiyama, S. *Nat. Nanotechnol.* **2007**, *2*, 401−410. (k) Pischel, U. *Angew. Chem., Int. Ed.* **2007**, *46*, 4026−4040. (l) Credi, A. *Angew. Chem., Int. Ed.* **2007**, *46*, 5472−5475.

(3) de Silva, A. P.; Gunaratne, H. Q. N.; McCoy, C. P. *Nature* **1993**, *364*, 42−44.

(4) (a) Ghosh, P.; Bharadwaj, P. K. *J. Am. Chem. Soc.* **1996**, *118*, 1553−1554. (b) Collier, C. P.; Wong, E. W.; Belohradsky, M.; Raymo, F. M.; Stoddart, J. F.; Kuekes, P. J.; Williams, R. S.; Heath, J. R. *Science* **1999**, *285*, 391−394.

(5) de Silva, A. P.; McClenaghan, N. D. *Chem.—Eur. J.* **2002**, *8*, 4935−4945.

(6) (a) Credi, A.; Balzani, V.; Langford, S. J.; Stoddart, J. F. *J. Am. Chem. Soc.* **1997**, *119*, 2679−2681. (b) Matsui, J.; Mitsuishi, M.; Aoki, A.; Miyashita, T. *J. Am. Chem. Soc.* **2004**, *126*, 3708−3709.

(7) (a) Lee, S. H.; Kim, J. Y.; Kim, S. K.; Leed, J. H.; Kim, J. S. *Tetrahedron* **2004**, *60*, 5171−5176. (b) Tang, Y.; He, F.; Wang, S.; Li, Y.; Zhu, D.; Bazan, G. C. *Adv. Mater.* **2006**, *18*, 2105−2110.

(8) (a) Montenegro, J.-M.; Perez-Inestrosa, E.; Collado, D.; Vida, Y.; Suau, R. *Org. Lett.* **2004**, *6*, 2353−2355. (b) Guo, X.; Zhang, D.; Tao, H.; Zhu, D. *Org. Lett.* **2004**, *6*, 2491−2494. (c) Straight, S. D.; Andréasson, J.; Kodis, G.; Bandyopadhyay, S.; Mitchell, R. H.; Moore, T. A.; Moore, A. L.; Gust, D. *J. Am. Chem. Soc.* **2005**, *127*, 9403−9409. (d) Qu, D. H.; Ji, F. Y.; Wang, Q. C.; Tian, H. *Adv. Mater.* **2006**, *18*, 2035−2038.

(9) de Sousa, M.; de Castro, B.; Abad, S.; Miranda, M. A.; Pischel, U. *Chem. Commun.* **2006**, 2051−2053.

(10) Baytekin, H. T.; Akkaya, E. U. *Org. Lett.* **2000**, *2*, 1725−1727.

(11) (a) de Silva, A. P.; McClenaghan, N. D. *J. Am. Chem. Soc.* **2000**, *122*, 3965−3966. (b) Andréasson, J.; Kodis, G.; Terazono, Y.; Liddell, P. A.; Bandyopadhyay, S.; Mitchell, R. H.; Moore, T. A.; Moore, A. L.; Gust, D. *J. Am. Chem. Soc.* **2004**, *126*, 15926−15927. (c) Qu, D.-H.; Wang, Q.-C.; Tian, H. *Angew. Chem., Int. Ed.* **2005**, *44*, 5296−5299. (d) Remacle, F.; Weinkauf, R.; Levine, R. D. *J. Phys. Chem. A* **2006**, *110*, 177−184. (e) Zhou, Y.; Wu, H.; Qu, L.; Zhang, D.; Zhu, D. *J. Phys. Chem. B* **2006**, *110*, 15676−15679. (f) Margulies, D.; Melman, G.; Felder, C. E.; Arad-Yellin, R.; Shanzer, A. *J. Am. Chem. Soc.* **2004**, *126*, 15400−15401. (g) Langford, S. J.; Yann, T. *J. Am. Chem. Soc.* **2003**, *125*, 11198−11199. (h) Coskun, A.; Deniz, E.; Akkaya, E. U. *Org. Lett.* **2005**, *7*, 5187−5189. (i) Liu, Y.; Jiang, W.; Zhang, H.-Y.; Li, C.-J. *J. Phys. Chem. B* **2006**, *110*, 14231−14235. (j) Suresh, M.; Jose, D. A.; Das, A. *Org. Lett.* **2007**, *9*, 441−444.

(12) Stojanovic, M. N.; Stefanovic, D. *Nat. Biotechnol.* **2003**, *125*, 6673−6676.

(13) (a) Mano, M. M.; Kime, C. R.; Kime, C. *Logic and Computer Design Fundamentals*, 3rd ed.; Prentice Hall: New Jersey, 2003. (b) Pippenger, D. E.; Tobaben, E. J.; McCollum, C. L. *Linear and Interface Circuits Applications*; Texas Instruments Inc.: Dallas, TX, 1986.

(14) Guo, Z.; Zhu, W.; Shen, L.; Tian, H. *Angew. Chem., Int. Ed.* **2007**, *46*, 5549−5553.

(15) (a) Valeur, B.; Leray, I. *Coord. Chem. Rev.* **2000**, *205*, 3−40. (b) Maruyama, S.; Kikuchi, K.; Hirano, T.; Urano, Y.; Nagano, T. *J. Am. Chem. Soc.* **2002**, *124*, 10650−10651. (c) Peng, X.; Du, J.; Fan, J.; Wang, J.; Wu, J.; Wu, Y.; Zhao, J.; Sun, S.; Xu, T. *J. Am. Chem. Soc.* **2007**, *129*, 1500−1501.

(16) Bourson, J.; Valeur, B. *J. Phys. Chem.* **1989**, *93*, 3871−3876.

(17) (a) Guo, X.; Qian, X.; Jia, L. *J. Am. Chem. Soc.* **2004**, *126*, 2272−2273. (b) Hirano, T.; Kikuchi, K.; Urano, Y.; Higuchi, T.; Nagano, T. *J.*

Am. Chem. Soc. **2000**, *122*, 12399−12400. (c) Woodroofe, C. C.; Lippard, S. J. *J. Am. Chem. Soc.* **2003**, *125*, 11458−11459. (d) Tang, B.; Huang, H.; Xu, K.; Tong, L.; Yang, G.; Liu, X.; An, L. *Chem. Commun.* **2006**, 3609−3611.

(18) Suzuki, Y.; Yokoyama, K. *J. Am. Chem. Soc.* **2005**, *127*, 17799−17802.

(19) (a) Pross, A.; Radom, L.; Taft, R. *J. Org. Chem.* **1980**, *45*, 818−826. (b) Rappoport, Z. *The Chemistry of Phenols*; John Wiley & Sons: Chichester, 2003.

(20) Yang, R.; Li, K.; Wang, K.; Zhao, F.; Li, N.; Liu, F. *Anal. Chem.* **2003**, *75*, 612−621.

(21) (a) de Costa, M. D. P.; de Silva, A. P.; Pathirana, S. T. *Can. J. Chem.* **1987**, *65*, 1416−1419. (b) Hermann, R.; Mahalaxmi, G. R.; Jochum, T.; Naumov, S.; Brede, O. *J. Phys. Chem. A* **2002**, *106*, 2379−2389.

(22) http://semiconductors.globalspec.com/ProductFinder/Semiconductors_Electronics/Digital_Logic_Devices.

(23) https://www.cs.tcd.ie/courses/baict/baca/jf/1ICT4-NOTES.pdf.

(24) Woods, L. L. *J. Am. Chem. Soc.* **1958**, *80*, 1440−1442.